Characterisation of the heterogeneity of a sand specimen in triaxial compression using x-ray CT and representative elementary volumes

Selma Schmidt[1#], *Max* Wiebicke[2], and *Ivo* Herle[1]

[1]*Technische Universität Dresden, Institut für Geotechnik, George-Bähr Strasse 1a, Dresden 01069, Germany*
[2]*The University of Sydney, Sydney Centre in Geomechanics and Mining Materials, Sydney 2006, Australia*
[#]*Corresponding author: selma.schmidt@tu-dresden.de*

ABSTRACT

Standard laboratory tests, such as the triaxial test, are often considered to be element tests. But, when observing such a test, it becomes obvious that this assumption of homogeneity is far from accurate. The localisation of strain is often visible to the naked eye and becomes even more obvious when observed on the grain scale. Other variables, such as those describing the soil fabric, are expected to localise as well. In this work, two sand samples are analysed at different loading states regarding the heterogeneity of three soil variables: void ratio, coordination number and contact orientation anisotropy. For this purpose, the size of a Representative Elementary Volume (REV) is determined using three criteria: the convergence of the mean and variance of the variables with increasing element size as well as a χ^2-test. The size of the REV is varying depending on the chosen variable but almost the same for the two specimens when related to the mean grain diameter d_{50}. The REV is placed in a regular grid throughout the specimen and the three variables are determined for each REV. The stochastic as well as spatial heterogeneity is identified for each specimen. As one of the samples is analysed for different loading states throughout a triaxial test, the evolution of the soil heterogeneity is identified. A localisation of all three variables can be observed at the end of the triaxial test as well as a strong initial heterogeneity for both sand samples.

Keywords: REV; contact fabric; heterogeneity; x-ray CT.

1. Introduction

The constitutive modelling of soils and the calibration of such soil models assumes of homogeneity. Standard laboratory tests used to calibrate the soil parameters embedded in the constitutive equations are therefore considered to be element test, meaning that the specimen is assumed to behave homogeneously and thus represents a material point.

This assumption contradicts the observations that can often be made during element tests, such as the triaxial test: the formation of one or multiple shear bands. Sometimes, those shear band patterns can be so complex that they stretch along the entire specimen but, at the same time, are concealed by their symmetry and thus not visible from the outside. This observation was first made by Desrues et al. (1996) studying different triaxially compressed Hostun sand samples with the help of x-ray computed tomography (CT).

Since then, x-ray CT and especially micro-focus CT (µCT) have been widely used to analyse the micro-structure of soils and confirming the observation of heterogeneity. This heterogeneity can already be found at a very early stage of the test, perhaps even at the initial state (Desrues et al. 2018). It was found that oftentimes, micro shear bands form at the beginning of the test and evolve into a wider globally visible shear band (Amirrahmat et al. 2019).

These findings certainly contradict the assumption of homogeneity. It is obvious that the heterogeneous state of the soil must be considered as Wood (2012) points out that *"the heterogeneous state is the natural state of granular materials"*. He emphasizes that *"the dimensions hidden in the patterns of heterogeneity are the ones that should be of concern in studying the mechanical response of such materials"*. This raises the question of dimension and size and ultimately that of a representative elementary volume (REV).

There is a great variety of definitions for the REV and multiple ways to determine its size. Al-Raoush and Papadopoulos (2010) define the REV as *"the minimum volume of a soil sample from which a given parameter becomes independent of the size of the sample"* and Wiącek and Molenda (2016) point out that its size depends on the analysed variable.

In order to determine the size of the REV from a CT scan of a soil specimen, elements with increasing size are extracted from a certain region of the specimen. In most cases, the REV size is identified by analysing the convergence of the porosity (Razavi, Muhunthan, and Hattamleh 2006) or local void ratio (Imseeh, Alshibli, and Al-Raoush 2020) of one element. As an additional criterion, Gitman, Askes, and Sluys (2007) introduced the χ^2-test.

A reliable determination of the REV size is achieved by extracting elements from different regions of the specimen and analysing the convergence of the mean and the variance of a chosen variable with increasing element size as well as performing a χ^2-test (Schmidt, Wiebicke, and Herle 2022). By placing the REV in a regular grid throughout the specimen, the soil heterogeneity becomes visible. It has been found that not only the void ratio localises when a shear band forms inside the specimen but also the contact fabric.

The fabric of the soil is characterised by the position and orientation of e.g. grains, contacts or voids and can be described by a fabric tensor. Its evolution has been studied multiple times (Fonseca et al. 2013; Imseeh, Druckrey, and Alshibli 2018; Wiebicke et al. 2020; Ganju et al. 2021) as it is closely connected to the overall behaviour of the soil. In order to form a connection between the microscopic evolution of the soil fabric and its macroscopic response, the discrete element method can be used to establish a stress-force-fabric relationship (Sufian, Russell, and Whittle 2017; Jiang, Zhang, and Li 2019).

The extraction of fabric quantities from CT images requires a careful image analysis and reliable tools. Wiebicke et al. first evaluated common image analysis tool regarding their accuracy (2017) and then developed a benchmark strategy to assess their ability to determine contact fabric from CT images (2019). Based on their findings, they proposed a procedure to reliably obtain contact fabric, which is also used in this work.

The objective of this work is the introduction and application of a method to determine the size of the REV for three variables (void ratio, coordination number and contact orientation anisotropy) and to analyse the heterogeneity of the specimen regarding these variables. One Hostun sand sample is studied throughout a triaxial test and compared to a Silica sand sample with respect to the REV size as well as the variation of the variables inside the specimen.

2. Preparation of the µCT images

2.1. Sample and test description

The Hostun sand sample analysed in this work was first described by Wiebicke et al. (2020). Further information on the test conditions and the x-ray scans can also be found there. 13 µCT images have been acquired at different loading states throughout a triaxial test at 100 kPa cell pressure. The sample has been pluviated and was initially dense. The first µCT-image has been obtained after isotropically compressing the dry specimen to a pressure of 100 kPa, which is here referred to as the initial state. Hostun sand has a narrow grain size distribution with a mean grain diameter d_{50} = 338 µm and angular particles. The specimen size was d = 11 mm and h = 22 mm and the voxel size of the CT image 15 µm.

A detailed description of the Silica sand sample has been given by Bacic and Herle (2020). The sample has been prepared by underwater pluviation which leads to an initially loose/medium dense state. The µCT-image has been acquired after applying a small negative pore water pressure for the stability of the specimen. Silica sand also has a narrow grain size distribution, but a mean grain diameter d_{50} = 943 µm and more rounded particles. The size of the specimen was d = 20 mm and h = 40 mm in this case and the voxel size of the CT image 12.5 µm.

2.2. Image analysis

The CT images have been analysed using the procedure developed by Wiebicke et al. (2020) and the open-source software *spam* (Stamati et al. 2020): The images are first binarised by a global threshold, namely Otsu's threshold, and then segmented by a topological watershed. When analysing the contacts between grains, image defects, such as the image noise or the partial volume effect, greatly influence the accuracy of contact detection and contact orientation determination. Wiebicke et al. (2017) proposed some enhancements of the image analysis procedure to face these issues, which are also implemented here. In order to detect contacts more reliably, a local threshold is introduced. The calculation of the contact orientation is enhanced by applying a power watershed, namely the random walker, which allows for the determination of the contact area on a sub-pixel level. Over-segmentation is handled by defining a maximum contact area. The contact orientation is calculated by performing a principal component analysis which requires the contact area to be composed of a minimum number of voxels.

The three variables analysed in this work are the void ratio e, the coordination number Z and the contact orientation anisotropy a. The void ratio can be calculated from the solid volume V_s and overall volume V of the specimen, both determined through voxel counting, the former using the original image and the latter using an image with filled holes. The pore volume V_p can then be calculated from these two values:

$$e = \frac{V_p}{V_s} = \frac{V - V_s}{V_s} \quad (1)$$

The coordination number describes the average number of contacts per grain and is defined as:

$$Z = \frac{2 \cdot N_c}{N_p} \quad (2)$$

with N_c being the number of contacts and N_p the number of particles. The contact orientation anisotropy is calculated from the deviatoric part **D** of the second order fabric tensor **N**

$$a = \sqrt{\frac{3}{2} \boldsymbol{D} : \boldsymbol{D}} \quad (3)$$

$$\boldsymbol{N} = \frac{1}{N} \sum_{\alpha=1}^{N} \boldsymbol{o}^{\alpha} \otimes \boldsymbol{o}^{\alpha} \quad (4)$$

with N being the number of orientations and **o** being one individual orientation.

3. Size of the Representative Elementary Volume (REV)

3.1. Hostun sand specimen

For the analysis of the soil heterogeneity regarding the three chosen variables, it is necessary to find a representative element. As described above, to reliably determine the size of the REV, three criteria are combined: the convergence of the mean and the variance

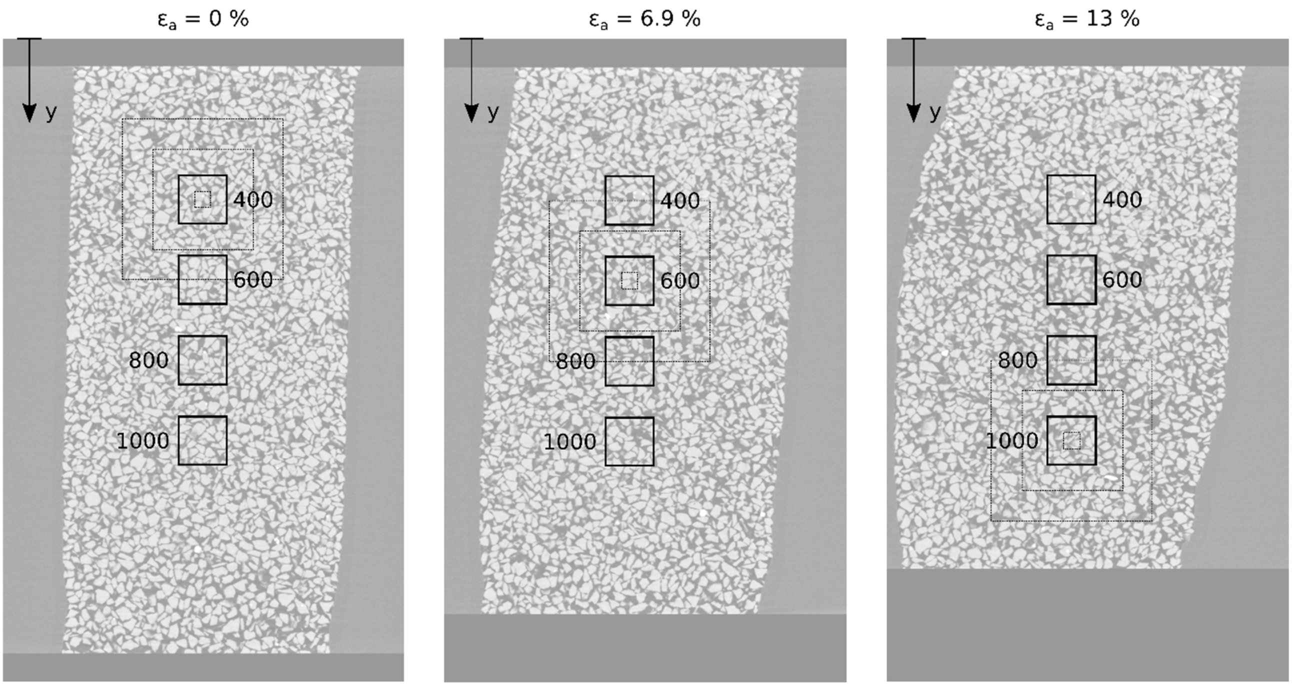

Figure 1. Positions of elements for the determination of the REV size for the Hostun sand specimen.

of a variable and a χ^2-test. The mean value of a variable can be calculated as

$$\bar{a} = \frac{1}{r}\sum_{i=1}^{r} a_i \quad (5)$$

where a_i are the values of that variable at r different positions inside the specimen. The variance is then calculated as

$$\sigma^2 = \frac{1}{r}\sum_{i=1}^{r}(a_i - \bar{a})^2 \quad (6)$$

The χ^2-value is defined as

$$\chi^2 = \sum_{i=1}^{r}\frac{(a_i - \bar{a})^2}{\bar{a}} \quad (7)$$

and the critical value for the χ^2-test corresponds to the degrees of freedom k = r – m – 1 with m being the number of estimated parameters.

For the determination of the REV size of the Hostun sand sample, elements are extracted from four positions along the vertical centre line of the specimen. The element positions are visualized in Fig. 1 at different loading states of the specimen. The number next to the element refers to the y-coordinate of the element centre in voxels. They are fixed throughout the whole triaxial test. The element size is increased subsequently and for each element, the void ratio e, coordination number Z and anisotropy a are calculated.

The evolution of the values with increasing element size (with reference to the mean grain diameter d_{50}) is plotted in Fig. 2 for the initial state in terms of mean and variance as well as for each individual position. The χ^2-value is displayed as well. The degrees of freedom for the χ^2-test is k = 2 as the number of element positions is r = 4 and only the mean value is estimated (m = 1). One critical value is chosen for all three variables and all loading states before localization ($\chi^2_{crit} = 0.103$) and then re-calibrated for all loading states after the onset of localization ($\chi^2_{crit} = 0.211$).

For each of the loading states, the three criteria are evaluated individually for each variable and the maximum size given by one of the criteria is then chosen to be the REV size. For example, at the initial state (Fig. 2) the χ^2-test would suggest a REV size of 2.66 d_{50} for the anisotropy but the mean value does not converge until 3.55 d_{50}. The REV sizes for the coordination number and the void ratio are determined analogously leading to the final REV sizes of 3.55 d_{50} for the anisotropy and the coordination number and 2.66 d_{50} for the void ratio at the initial state. This procedure is repeated for every loading state. The maximum REV sizes considering all states of the Hostun sand sample are 5.33 d_{50} for the anisotropy and the coordination number and 3.55 d_{50} for the void ratio. Those are also the sizes used for the analysis of the heterogeneity.

3.2. Silica sand specimen

The REV size for the Silica sand sample is determined analogously to the Hostun sand sample. Elements with increasing size are extracted from four positions along the vertical centre line of the specimen, which are also shown in Fig. 3. The convergence of the mean and the variance of the three chosen variables is evaluated as well as a χ^2-test. For the Silica sand sample, only the initial state is analysed. The evolution of the void ratio, the coordination number and the anisotropy with increasing element size in terms of mean and variance as well as for each individual position is displayed in Fig. 4. The element sizes are related to the mean grain diameter d_{50} to allow a better comparison with the Hostun sand sample. The χ^2-test is shown on the bottom. The critical value is chosen to be the same as for the initial state of the Hostun sand sample, which is $\chi^2_{crit} = 0.103$.

The REV sizes are again evaluated for each variable individually and the maximum size given by one of the criteria is defined as the size of the REV. For example, the χ^2-test suggests a REV size of 2.39 d_{50} for the

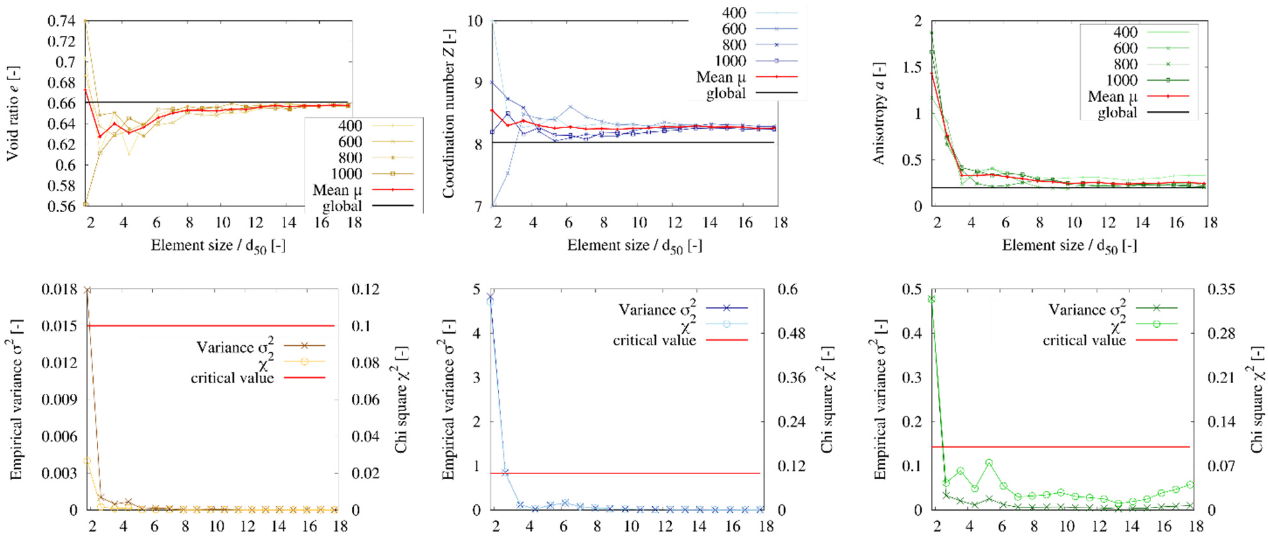

Figure 2. Determination of the REV size for the Hostun sand specimen.

coordination number, but as the variance does not converge until 3.45 d_{50}, this size is chosen to be the REV size. This is done analogously for the other two variables leading to the final REV sizes of 3.45 d_{50} for the coordination number and the anisotropy and 2.92 d_{50} for the void ratio.

It has to be noted that especially for the Silica sand specimen, the mean value of the four analysed elements does not approach the global value. This is a result of the heterogeneity of the specimen and the fact that the four locations have been chosen randomly.

In Table 1, the REV size for the two sand samples at the initial state are compared. As the REV size is referred to the mean grain diameter d_{50}, the different grain sizes of the two sands do not influence the results. In general, the sizes of the REVs for the three analysed variables are very similar. It is also striking that, for both samples, the REV size is the same for the two variables describing the contact fabric and smaller for the void ratio. This might reflect the higher sensitivity of the contact fabric towards changes inside the specimen compared to the void ratio.

Table 1. REV sizes at the initial state [d_{50}]

	Void ratio	Coord. Number	Anisotropy
Hostun sand	2.66	3.55	3.55
Silica sand	2.92	3.45	3.45

4. Analysis of the heterogeneity with the REV

4.1. Hostun sand specimen

The heterogeneity of the soil samples is now analysed by placing the REV in a regular grid throughout the whole specimen. A fine grid is chosen for a more detailed analysis of the heterogeneity. For each element, the void ratio, the coordination number and the anisotropy are determined. REVs that lie on the border of the specimen need to be checked regarding their representativity. A threshold is defined for the two contact fabric variables with respect to the number of particles and for the void ratio with respect to the total soil volume (particles and internal voids) inside the element. The former threshold is chosen based on the number of particles that can be found in REVs inside the specimen and the latter one is defined on the basis of the analysis of the REV size.

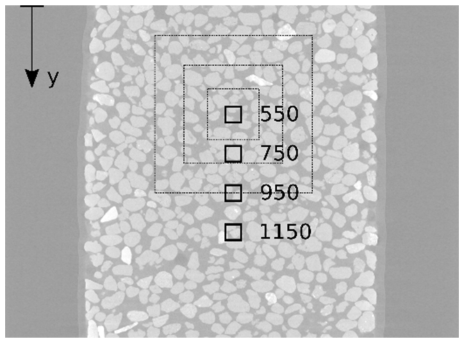

Figure 3. Positions of elements for the determination of the REV size for the Silica sand specimen.

The Hostun sand sample is analysed with a REV size of 5.33 d_{50} for the anisotropy and the coordination number and 3.55 d_{50} for the void ratio, which are the sizes determined over all loading states. To count as a REV, 90 particles are defined as the threshold value for boundary elements regarding the contact fabric variables. For the void ratio, 68% of the element needs to be filled with soil.

The initial and final heterogeneity of the Hostun sand sample can be seen in Fig. 5. Especially for the anisotropy, a large variation inside the specimen can already be observed at the initial state. On average, the values scatter 30.3% around the mean value. The coordination number and the void ratio also show an initial heterogeneity but not to this extent. The anisotropy is greatly influenced by very small changes of the contact fabric as it is not only impacted by the re-orientation but also by the loss and gain of contacts. This might be one of the reasons for the large initial scatter.

At the final state of the triaxial test, the localisation zone becomes clearly visible. It is wider for the anisotropy than for the other two variables underlining the high sensitivity of this variable leading to a broader area influenced by the localisation. The coordination

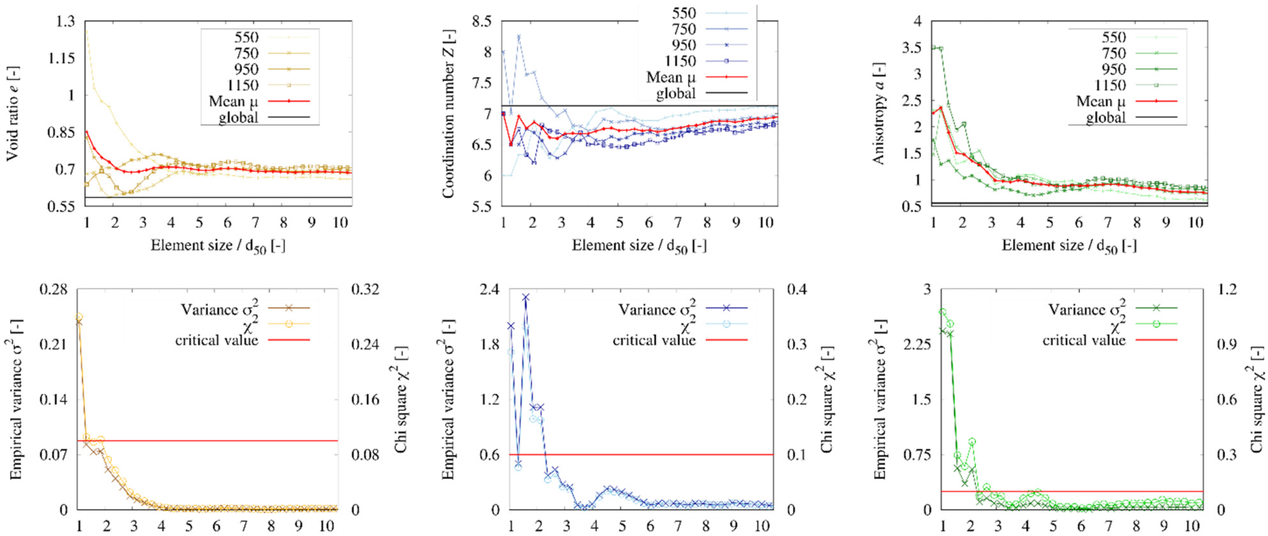

Figure 5. Determination of the REV size for the Silica sand specimen.

number also has a wider localisation zone than the void ratio indicating an overall higher sensitivity of the contact fabric towards changes inside the specimen in comparison to standard soil variables.

4.2. Silica sand specimen

For the Silica sand specimen, only the initial state was analysed and is displayed in Fig. 6. The mean initial anisotropy is much greater than for the initial state of the Hostun sand sample with a value of a = 0.73 compared to a = 0.36. This is probably due to the specimen preparation where the grains are poured into a cone. For the anisotropy, one can also observe some localisation zones inside the specimen already at the initial state which might result from the specimen preparation as well. On average, the anisotropy deviates 32.8% around the mean value, which is around the same value as for the Hostun sand sample.

In contrast, the scatter of the void ratio, with 9.8% and the coordination number with 5.5% average deviation around the mean is larger than for the Hostun sand with 4.2% and 2.3%, respectively. This could mostly be a result of the different specimen density as the Silica sand sample is generally looser allowing for a higher scatter in void space and contact distribution. For these two variables, one can also identify some localisation zones but they have not fully formed yet, as opposed to the one visible for the anisotropy.

In general, the initial state of both analysed soil samples regarding the void ratio, the coordination number and the anisotropy is clearly not homogeneous. The initial deviation of the three variables is summarised in Table 2. The extremely large scatter of the anisotropy at the initial state compared to the other two variables is striking.

Table 2. Mean values and standard deviation of the three analysed variables at the initial state

	Void ratio	Coord. number	Anisotropy
Hostun sand	0.66 (4.2%)	8.23 (2.3%)	0.36 (30.3%)
Silica sand	0.65 (9.8%)	7.10 (5.5%)	0.73 (32.8%)

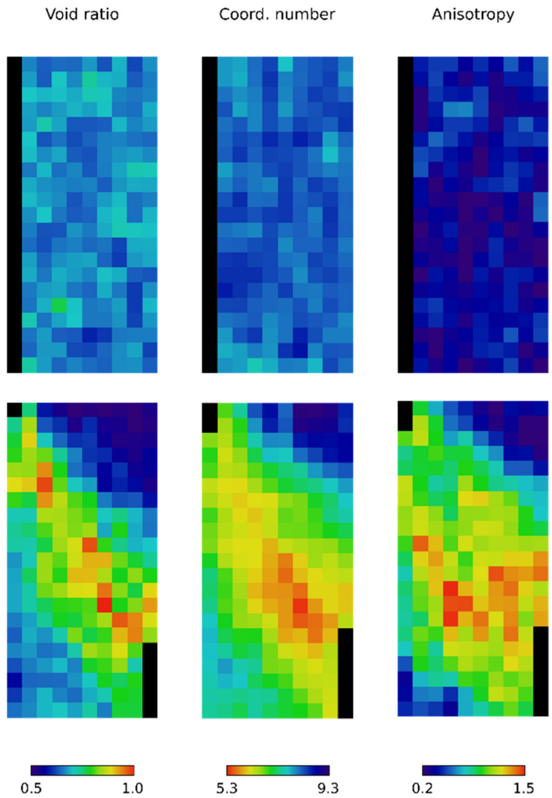

Figure 4. Heterogeneity of the three analysed variables at the initial and final state of the Hostun sand specimen. Excluded boundary elements are visualised in black.

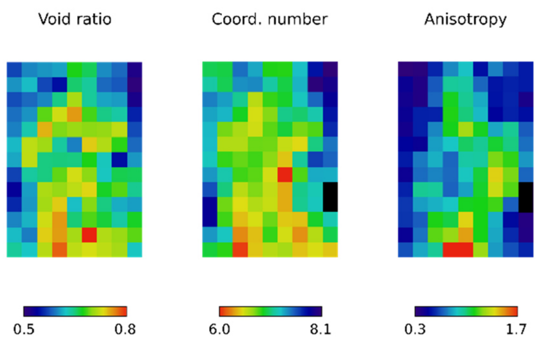

Figure 6. Heterogeneity of the three analysed variables at the initial state of the Silica sand specimen.

5. Conclusions

The heterogeneity of two sand samples, one Hostun sand sample and one Silica sand sample, has been analysed regarding the void ratio and two contact fabric descriptors, namely the coordination number and the anisotropy. For this purpose, the size of a representative elementary volume has been determined using the procedure from Schmidt, Wiebicke, and Herle (2022). Three criteria have been used to reliably find the REV. The heterogeneity has been analysed by placing the REV in a regular grid throughout the specimen. The main findings of this analysis are summed up below:

- The REV sizes, with reference to the mean grain diameter d_{50}, are very similar for the two sands at the initial state. The REVs of the two contact fabric variables have the same size and are larger than the one determined for the void ratio.
- There is already a strong initial heterogeneity for both samples, especially regarding the anisotropy. The initial deviation of the void ratio and the coordination number is larger for the looser sample, i.e. the Silica sand sample, but for both samples much smaller than the deviation of the anisotropy.
- The sample preparation method for the Silica sand sample leads to a higher initial anisotropy and the formation of initial localisation zones.
- Throughout the triaxial test, one localisation zone forms inside the Hostun sand sample, which becomes visible for all three variables. The localisation width is different for the variables: the widest zone develops for the anisotropy as this is the most sensitive one towards changes inside the specimen and the void ratio has the narrowest localisation zone.

These results emphasise the importance of considering the heterogeneity of the soil. It is shown that we can expect a strong heterogeneity already at the initial state, especially regarding the contact orientation anisotropy. The importance of the analysis of the contact fabric has been underlined as it is much more sensitive to changes inside the specimen than standard soil variables such as the void ratio and can therefore detect them early.

To better understand the influences on the soil heterogeneity, further investigations need to be made with a greater variety of samples. The dependence of the REV size on soil properties such as particle size distribution and grain shape also need further examination. All in all, we must find new ways to define the soil properties other than by assuming homogeneity, which clearly does not reflect the reality.

Acknowledgements

We thank Pascal Charrier, Edward Andò and Gioacchino Viggiani from Laboratoire 3SR as well as Martin Oppermann from ZmP for the allocation of time and comprehensive support for the x-ray scanners.

We thank the Centre for Information Services and High Performance Computing (ZIH) at TU Dresden for generous allocations of computing resources.

We thank the German Research Foundation (DFG) for the funding of the research leading to this results, Grant No. 453596084 (SFB/TRR 339).

References

Al-Raoush, R., A. Papadopoulos. 2010. "Representative elementary volume analysis of porous media using X-ray computed tomography" Powder Technology 200, no. 1-2: 69-77. https://doi.org/10.1016/j.powtec.2010.02.011

Amirrahmat, S., A. M. Druckrey, K. A. Alshibli, R. I. Al-Raoush. 2019. "Micro Shear Bands: Precursor for Strain Localization in Sheared Granular Materials" J Geotech Geoenviron Eng 145, no. 2: 04018104. http://dx.doi.org/10.1061/(ASCE)GT.1943-5606.0001989

Bacic, B., I. Herle. 2020. "A simple method for the determination of sensitivity to density changes in sand liquefaction" Open Geomechanics 2, 1–8. https://doi.org/10.5802/ogeo.6

Desrues, J., E. Andò, F. A. Mevoli, L. Debove, G. Viggiani. 2018. "How does strain localise in standard triaxial tests on sand: Revisiting the mechanism 20 years on" Mechanics Research Communications 92, 142–146. https://doi.org/10.1016/j.mechrescom.2018.08.007

Desrues, J., R. Chambon, M. Mokni, F. Mazerolle. 1996. "Void ratio evolution inside shear bands in triaxial sand specimens studied by computed tomography" Géotechnique 46, no. 3: 529–546. https://doi.org/10.1680/geot.1996.46.3.529

Fonseca, J., C. O'Sullivan, M. R. Coop, P. Lee. 2013. "Quantifying the evolution of soil fabric during shearing using directional parameters" Géotechnique 63, no. 6: 487–499. https://doi.org/10.1680/geot.12.P.003

Ganju, E., M. Kılıç, M. Prezzi, R. Salgado, N. Parab, W. Chen. 2021. "Effect of particle characteristics on the evolution of particle size, particle morphology, and fabric of sands loaded under uniaxial compression" Acta Geotech 16, no. 11: 3489–3516. https://doi.org/10.1007/s11440-021-01309-3

Gitman, I., H. Askes, L. Sluys. 2007. "Representative volume: Existence and size determination" Engineering fracture mechanics 74, no. 16: 2518–2534. https://doi.org/10.1016/j.engfracmech.2006.12.021

Imseeh, W. H., K. A. Alshibli, R. I. Al-Raoush. 2020. "Discrepancy in the Critical State Void Ratio of Poorly Graded Sand due to Shear Strain Localization" J Geotech Geoenviron Eng 146, no. 8: 04020066. https://doi.org/10.1061/(asce)gt.1943-5606.0002280

Imseeh, W. H., A. M. Druckrey, K. A. Alshibli. 2018. "3D experimental quantification of fabric and fabric evolution of sheared granular materials using synchrotron micro-computed tomography" Granular Matter 20, no. 2: 1–28. https://doi.org/10.1007/s10035-018-0798-x

Jiang, M., A. Zhang, T. Li. 2019. "Distinct element analysis of the microstructure evolution in granular soils under cyclic loading" Granular Matter 21, no. 2: 1–16. https://doi.org/10.1007/s10035-019-0892-8

Razavi, M. R., B. Muhunthan, O. Al Hattamleh. 2006. "Representative Elementary Volume Analysis of Sands Using X-Ray Computed Tomography" Geotech Test J 30, no. 3: 212-219. https://doi.org/10.1520/GTJ100164

Schmidt, S., M. Wiebicke, I. Herle. 2022. "On the determination and evolution of fabric in representative elementary volumes for a sand specimen in triaxial compression" Granular Matter 24, no. 4: 1–9. https://doi.org/10.1007/s10035-022-01262-2

Stamati, O., E. Andò, E. Roubin, R. Cailletaud, M. Wiebicke, G. Pinzon, C. Couture, R. C. Hurley, R. Caulk, D. Caillerie, et al. 2020. "spam: Software for practical analysis of materials" JOSS 5, no. 51: 2286. https://dx.doi.org/10.21105/joss.02286

Sufian, A., A. Russell, A. Whittle. 2017. "Anisotropy of contact networks in granular media and its influence on mobilised internal friction" Géotechnique 67, no. 12: 1067–1080. https://doi.org/10.1680/jgeot.16.P.170

Wiącek, J., M. Molenda. 2016. "Representative elementary volume analysis of polydisperse granular packings using discrete element method" Particuology 27, 88–94. https://doi.org/10.1016/j.partic.2015.08.004

Wiebicke, M., E. Andò, I. Herle, G. Viggiani. 2017. "On the metrology of interparticle contacts in sand from x-ray tomography images" Meas Sci Technol 28, no. 12: 124007. https://doi.org/10.1088/1361-6501/aa8dbf

Wiebicke, M., E. Andò, V. Šmilauer, I. Herle, G. Viggiani. 2019. "A benchmark strategy for the experimental measurement of contact fabric" Granular Matter 21, no. 3: 1–13. https://doi.org/10.1007/s10035-019-0902-x

Wiebicke, M., E. Andò, G. Viggiani, I. Herle. 2020. "Measuring the evolution of contact fabric in shear bands with x-ray tomography" Acta Geotech 15, no. 1: 79–93. https://doi.org/10.1007/s11440-019-00869-9

Wood, D. M. 2012. "Heterogeneity and soil element testing" Géotechnique Letters 2, no. 3: 101–106. https://doi.org/10.1680/geolett.12.00019